Title page

Title: Accuracy of periodontal bone loss assessed by three-dimensional periodontal ligament models using cone-beam computed tomography at different resolutions

Authors' name and information

Hangmiao Lyu[1], Li Xu[2], Huimin Ma[1], Jianxia Hou[2], Xiaoxia Wang[3], Yong Wang[4], Yijiao Zhao[4], Weiran Li[1], Xiaotong Li[1]

[1]Department of Orthodontics, National Engineering Laboratory for Digital and Material Technology of Stomatology; Beijing Key Laboratory of Digital Stomatology, Peking University School and Hospital of Stomatology, 22 Zhongguancun Avenue South, Haidian District, Beijing, 100081, People's Republic of China.

[2]Department of Periodontology, National Engineering Laboratory for Digital and Material Technology of Stomatology; Beijing Key Laboratory of Digital Stomatology, Peking University School and Hospital of Stomatology, Haidian District, Beijing, 100081, People's Republic of China.

[3]Department of Oral and Maxillofacial Surgery, National Engineering Laboratory for Digital and Material Technology of Stomatology; Beijing Key Laboratory of Digital Stomatology, Peking University School and Hospital of Stomatology, 22 Zhongguancun Avenue South, Haidian District, Beijing, 100081, People's Republic of China.

[4]Center of Digital Dentistry, Peking University School and Hospital of Stomatology; National Engineering Laboratory for Digital and Material Technology of Stomatology; Research Center of Engineering and Technology for Digital Dentistry of Ministry of Health; Beijing Key Laboratory of Digital Stomatology, Peking University School and Hospital of Stomatology, 22 Zhongguancun Avenue South, Haidian District, Beijing, 100081, People's Republic of China.

Corresponding authors and information

1, Weiran Li (DDS, PhD, Professor)

Department of Orthodontics, National Engineering Laboratory for Digital and Material Technology of Stomatology; Beijing Key Laboratory of Digital Stomatology, Peking University School and Hospital of Stomatology, No. 22 ZhongGuanCun Nandajie, HaiDian District, Beijing 100081, People's Republic of China.

Zip code:10080

Telephone number: 010-82195381

E-mail: weiranli2003@163.com; weiranli@bjmu.edu.cn

2, Xiaotong Li (DDS, PhD, Associate Professor)

Department of Orthodontics, National Engineering Laboratory for Digital and Material Technology of Stomatology; Beijing Key Laboratory of Digital Stomatology, Peking University School and Hospital of Stomatology, No. 22 ZhongGuanCun Nandajie, HaiDian District, Beijing 100081, People's Republic of China.

Zip code:100081

Telephone number: 010-82195739

E-mail: xiaotonglee@hotmail.com

Acknowledgement

This study was approved by the Biomedical Ethics Committee of the Peking University School and Hospital of Stomatology (approval number: PKUSSIRB-201839156). Trial registration: Chinese Clinical Trials Registry Platform of the World Health Organization, ChiCTR1900021778. Registered 9 March 2019, https://www.chictr.org.cn/hvshowproject.aspx?id=16082. Informed consent was obtained from every participant.

Funding: This study was supported by National Program for Multidisciplinary Cooperative Treatment on Major Diseases (PKUSSNMP-201902).

Full manuscript

Accuracy of periodontal bone loss assessed by three-dimensional periodontal ligament models using cone-beam computed tomography at different resolutions

Abstract

Objective: The present study aimed to introduce a method for obtaining three-dimensional (3D) digital models of the periodontal ligament (PDL) using 3D cone-beam computed tomography (CBCT) reconstruction and to evaluate the accuracy and agreement of the periodontal bone loss assessed by 3D PDL models.

Methods: CBCT data collected from four skeletal class III patients prior to periodontal surgery were reconstructed at 3 voxel sizes (0.2 mm, 0.25 mm and 0.3 mm), and 3D teeth and alveolar bone models were generated to obtain PDL digital models of the upper and lower anterior teeth. Linear measurements of the alveolar bone crest obtained during periodontal surgery were compared with digital measurements to examine the accuracy of the digital models. The agreement and reliability of the digital PDL models were analysed using intra- and interexaminer correlations and Bland–Altman plots.

Results: Digital models of the upper and lower anterior teeth, PDL and alveolar bone of four patients were successfully established. Linear measurements obtained from the 3D digital models were accurate compared with the measurements obtained intraoperatively, and there were no significant differences among different voxel sizes at different sites. High diagnostic coincidence rates were found for the upper anterior teeth, and high intra- and interexaminer agreement was found for the digital models.

Conclusions: Digital PDL models acquired by 3D CBCT reconstruction provide accurate and useful information regarding the alveolar crest morphology and allow reproducible measurements, which could assist clinicians to evaluate periodontal prognosis and determine an appropriate orthodontic treatment plan.

Keywords: Digital models; 3D reconstruction; Cone-beam computed tomography

Introduction

The periodontal ligament (PDL) is an aligned fibrous network anchored firmly to the tooth root cementum on one side and the alveolar bone of the jaw on the other side [1, 2] and can be represented by the root surface area (RSA) below the alveolar bone crest. The area of contact between tooth roots and the surrounding bone plays an important role in orthodontic and periodontal treatment. It has been proposed that the PDL and alveolar bone are functional units that undergo robust remodelling during orthodontic tooth movement [3]. Moreover, the PDL area is associated with the anchorage of teeth [4], and morphological changes in the PDL reflect the vertical bone level [5]. The complete absence of the PDL leads to the direct contact of bone with the cementum, and if more than 20% of the PDL is injured, abnormal attachment can occur after healing [6].

Quantification of the PDL area can help assess the severity of periodontal disease and the prognosis of orthodontic treatment.

The method for measuring the alveolar bone thickness and vertical bone level (VBL) on the sagittal plane of cone-beam computed tomography (CBCT) images has been well established [7-9]. Past studies have focused primarily on measuring the height and thickness of alveolar bone on the labial and lingual sides of the incisors on the sagittal plane. However, previous studies have found inconsistencies between three-dimensional (3D) measurements of the RSA of periodontal attachment and two-dimensional (2D) measurements of the VBL. Evaluating these 2D measurements without considering the 3D PDL area may not adequately indicate the severity of periodontal lesions. Moreover, 2D linear measurements describe the VBL in a one-dimensional manner without taking changes in the root shape into account, thus underestimating the true amount of periodontal loss [10-12].

Previous scholars have used a variety of methods to measure the RSA below the cementoenamel junction (CEJ) to represent the PDL area. However, these methods have disadvantages; for instance, they lack accuracy and require tooth extraction [13].

In other previous studies [10, 14], microcomputed tomography (micro-CT) data were used to measure the RSA on reconstructed digital models of extracted teeth. However, the micro-CT technique cannot be used in human patients for in situ examination because of the unacceptably high radiation exposure [15]. Unlike micro-CT [15, 16], CBCT provides data for accurate and reproducible 3D reconstruction of the tooth volume that are useful in some clinical applications. Additionally, CBCT combined with 3D reconstruction technology has been proven to be an efficient and reliable imaging technique for noninvasively acquiring data on tooth surfaces in vivo [16, 17]. Regarding the assessment of periodontal bone loss, measurements of periodontal defects obtained by CBCT combined with 3D reconstruction have shown very high agreement with measurements obtained intraoperatively [18] or by micro-CT, regardless of the voxel size [19].

Researchers have also reconstructed the root surface based on CBCT to detect apical root resorption cavities [16] and measure the RSA as an important marker for determination of the periodontal treatment plan and prognosis. However, RSA measurements do not take alveolar bone conditions into account; in recent years, the PDL surface area, or the RSA below the alveolar bone crest, has been studied to evaluate the periodontal health of teeth, and researchers have artificially simulated the PDL area using digital models of teeth in vitro [5, 10, 11, 14, 19]. Nevertheless, to date, no studies have performed alveolar bone crest-based 3D PDL area measurements in humans in vivo.

Instead of artificially simulating the alveolar bone crest in vitro, we measured the PDL area in vivo using 3D CBCT reconstruction. This study aimed to (1) utilize the 3D CBCT reconstruction technique to obtain 3D virtual models of the teeth, PDL, and alveolar bone, (2) evaluate the accuracy of the virtual models by

comparing digital measurements with direct intraoperative measurements, and (3) investigate the repeatability of the method.

Materials and Methods

Sample selection

Forty-eight anterior teeth from four patients (2 women, 2 men) with skeletal Class III malocclusion requiring surgical orthodontic treatment and augmented corticotomy (AC) surgery participated in the study at Peking University School and Hospital of Stomatology from May 2021 to October 2021. All patients signed informed consent forms. This study was approved by the Biomedical Ethics Committee of the Peking University School and Hospital of Stomatology (approval number: PKUSSIRB-201839156) and registered on the Clinical Trials Register as ChiCTR1900021778 (Chinese Clinical Trials Registry Platform of the World Health Organization).

The inclusion criteria were as follows: 1) age: male >18 years, female >16 years[20, 21]; 2) ANB angle < 0°, overjet < 0 mm; 3) periodontal health, with no more than two sites with a probing depth ≥ 5 mm among all teeth, bleeding on probing ≤ 20%, and plaque score ≤ 30%; and 4) labial alveolar bone thickness of upper or lower central incisors < 1 mm, as measured by CBCT. The mean alveolar bone thickness in this study at the root apex level of upper and lower central incisors were 0.81±0.17 mm and 0.4±0.15 mm, respectively.

Patients with poor oral hygiene or uncontrolled periodontal disease were excluded.

All orthodontic treatments were performed by a single orthodontist with a straight-wire fixed appliance (0.022" slot size, MBT prescription). For upper anterior teeth, the arch-wire sequence involved 0.014-, 0.016-, 0.018-, and 0.018×0.025-inch nickel-titanium wires before the periodontal surgery. For lower anterior teeth, periodontal surgery was performed on lower anterior teeth after bracket bonding without any arch wire in place. Two weeks after periodontal surgery, aligning and leveling started with 0.014-inch nickel-titanium wires.

Image acquisition

Prior to periodontal surgery, CBCT images were acquired with the NewTom VG device (Aperio Services, Italy) in regular scan mode (field of view (FOV), 10×10 cm; voltage, 110 kV; current, 3.00 mA; exposure, 1.8 seconds). The CBCT images were reconstructed using different voxel sizes (0.20, 0.25 and 0.30 mm). To reduce scatter at the occlusal plane, patients were instructed to bite on cotton rolls. Within 24 hours of taking CBCT, the patients also underwent an intraoral scan.

Method for obtaining digital models

DICOM files were imported into Mimics 19.0 software (Materialise, Leuven, Belgium). In Mimics, 3D digital models of the anterior teeth and bone in vivo were reconstructed. The teeth were segmented first, followed by the bone. In Mimics, the CBCT images had predefined thresholds that were set to correspond to the tooth or bone density: tooth, 1200-3071 segments; bone, 226-3071 segments. The threshold level was set

to most clearly show the tooth anatomy with minimal interference from the surrounding bone and adjacent structures. On each CBCT slice, manual refinement through a 2D slice-by-slice procedure to enhance accuracy by correcting for over- and under-contoured voxels in the tooth volume[22]. (Figure 1).

The digital models were exported in STL format and imported into Geomagic software (Geomagic, Cary, N.C.). For more realistic digitalization of the metal brackets bonded to the teeth, a digital model derived from the intraoral scan was superimposed over the 3D model generated from the CBCT datasets (Figure 2).

Linear measurements of the alveolar bone crest on CBCT-derived digital models

In Geomagic software (Geomagic, Cary, N.C.), the vertical distance between the CEJ and alveolar bone crest parallel to the long axis of the anatomic crown was defined as the VBL. The long axis of the anatomic crown was determined by connecting the lowest point of labial CEJ curve and the midpoint of the mesial and distal incisal angle. The five selected measurement sites on the digital models were the mesiolabial (VBL_MLa), mesiobracket (VBL_MB), midlabial (VBL_La), distobracket (VBL_DB), and distolabial (VBL_DLa) sites. The La point was chosen at the midlabial site on the surface. Proximal points on the surface, i.e., the MLa and DLa points, were located on the corner of each tooth. The vertical distance between the marginal bone crest and the gingival boundary of the metal bracket was defined as the bone-bracket distance (BBD). The three selected measurement points were the mesiobracket (BBD_MB), midlabial (BBD_La), and distobracket (BBD_DB) points. Detailed information about the measurement procedure is shown in Figure 3. Measurements were made to the nearest 0.01 mm with a linear measurement tool in a quiet and dark room.

Linear measurements of the alveolar bone crest during periodontal surgery

AC was performed by the same periodontist with surgical loupes. The AC procedure was as follows[23]: a crevicular incision was made from the canine on one side to the canine on the other side, and a full thickness flap on the labial side was elevated. The distance parallel to the long axis of the anatomic crown between the CEJ and the alveolar bone crest was measured at the five sites, as well as the distance between the alveolar bone crest and the gingival boundary at the mesial and distal metal bracket sites (Figure 4). All measurements were made to the nearest 1 mm by an experienced periodontist using a manual periodontal probe (UNC-15, graded in millimetres; HU-Friedy, Chicago, IL) parallel to the long axis of the tooth. The intraoperative measurements were regarded as the “reference standard”.

Method for segmenting the digital PDL

To segment the PDL in the digital model, we identified the alveolar bone crest on the bone in the digital model and drew points on the teeth in the model (Figure 5a, b). A curve was generated by connecting the points marked on the model surface using the creation method in Geomagic (Figure 5b). The created boundary curve represented the alveolar bone crest (Figure 5c). The teeth were then separated along the curve into two parts (Figure 5d), preserving the PDL (Figure 5e), and the area of the PDL in the digital model was calculated

(Figure 5f).

Statistical analysis

Statistical analyses were performed using SPSS 20.0 (IBM, Armonk, NY, USA). All linear measurements of the digital models were obtained twice at an interval of 2 weeks by the same investigator. The average of these two measurements was used for statistical analysis. The systematic intraexaminer error was determined using a paired t test, and the intraclass correlation coefficient (ICC) was calculated. One-way ANOVA with Duncan's multiple comparison test was performed to compare linear measurements obtained intraoperatively and by CBCT at different sites and with different voxel sizes, and the ICC was calculated. Moreover, the Bland–Altman method was applied, and the limits of agreement were identified.

Descriptive statistics for differences between the intraoperative and digital measurements were computed separately. In addition, the 95% confidence interval (CI) was calculated, and diagnostic coincidence rates were calculated via an introduced variable measurement difference to evaluate the accuracy of site-based image assessment compared with clinical measurement.

Measurement difference = intraoperative measurement—3D digital measurement

If the measurement difference ranged from -1 to 1 mm (including -1 and 1 mm), the measurement obtained from the 3D digital image was considered to be consistent with the intraoperative measurement; otherwise, the measurements were to be inconsistent. Then, the corresponding diagnostic coincidence rates were calculated. To examine the agreement of the digital models obtained by different examiners, 24 randomly chosen teeth were assessed in a blinded manner by two authors with between 4 and 8 years of experience in dental and periodontal imaging. The error was evaluated by measuring the surface area of the PDL in the models. The systematic interexaminer agreement was calculated using the ICC, and the Bland–Altman method was applied to identify the limits of agreement.

Results

Validation of 3D digital model accuracy and consistency according to voxel size

There were no significant differences in digital measurements of the upper anterior teeth at different sites among different voxel sizes ($P>0.05$) or in the VBL or BBD between the intraoperative and digital measurements ($P>0.05$) (Table 1).

There were no significant differences in digital measurements of the lower anterior teeth at different sites among different voxel sizes ($P>0.05$). Additionally, there were no significant differences between the digital and intraoperative BBD measurements ($P>0.05$). However, except for VBL_La, the digital VBL measurements were smaller than the intraoperative VBL measurements ($P<0.01$).

A statistically significant ICC was found between all digital and intraoperative measurements ($P<0.01$) (Table 2), with ICC values ranging from 0.646~0.793 for the VBL and 0.839~0.908 for the BBD.

Agreement and reliability of 3D virtual model measurements

The mean differences and descriptive statistics for the measurements are shown in Tables 3 and 4. The mean differences (and 95% CIs) between the digital and intraoperative measurements of the upper anterior teeth were approximately zero, confirming no significant differences. Statistically significant mean differences were found in the VBL measurements of the lower anterior teeth regardless of the voxel size ($P<0.01$), while the mean differences (and 95% CIs) of the BBD measurements were approximately zero.

The diagnostic coincidence rates of the VBL and BBD of the upper anterior teeth were ≥ 90%. For the lower anterior teeth, the diagnostic coincidence rates ranged from 56.66~63.33% for the VBL and 66.67~77.78% for the BBD (Tables 3 and 4).

To validate the different measurements, the differences between the digital and intraoperative measurements were plotted against the average as recommended in Bland–Altman analysis. The limits of agreement were defined as ±1.96*standard deviation (SD) and are shown in Figure 6. The limits of agreement of the upper anterior teeth showed discrepancies in the measurements of approximately 2 mm. However, high variability of measurements in the mandible was found, as indicated by the large 95% limits of agreement range of approximately 3.5 mm.

Intraexaminer agreement of linear measurements and interexaminer agreement of PDL area measurements

High intraexaminer agreement of linear measurements of the digital model was found. The results showed no statistically significant systematic intraexaminer error ($P>0.05$) and strong intraexaminer reliability (ICC = 0.985, 95% CI 0.973-0.991).

Differences in PDL area measurements between examiners were also analysed, and the results showed high interexaminer agreement (ICC = 0.947, 95% CI 0.871-0.979). Moreover, the Bland–Altman analysis showed good consistency between the 2 examiners in the process of segmenting the PDL in the model. The mean bias of the PDL area (mm^2) was 2.57, with limits of agreement from -17.89 to 23.03 (Figure 7), indicating good consistency between the 2 examiners in the process of PDL segmentation.

Establishment of PDL models

Digital models of the PDL of the upper and lower anterior teeth of four patients were established successfully, and an example from one of the patients is shown in Figure 8.

Discussion

The detection and monitoring of alveolar bone loss is important because it provides a hard-tissue index for the presence of periodontal disease and the effects of preventative and corrective therapies for periodontal disease [24, 25]. In the present study, we introduced a method to obtain alveolar bone crest -based digital PDL models using 3D CBCT reconstruction and designed an experiment to verify the accuracy of identifying the

alveolar crest and the consistency of PDL_Area measurements.

Previous studies have shown that CBCT provides data for accurate and reproducible 3D reconstruction of teeth that are useful in some clinical applications [15, 16, 26]. The present study suggests that 3D CBCT reconstruction also provides relatively accurate information regarding the alveolar bone of anterior teeth. There were no significant differences between measurements obtained using a CBCT voxel resolution of 0.20 mm, 0.25 mm, or 0.30 mm, which indicates the high value of this method for clinical application. Previous studies have shown that discernment of the PDL space requires CBCT data with a resolution capable of detecting structures less than 0.2 mm in size [24, 27]. However, higher-resolution data may require higher levels of radiation, which would increase the radiation exposure of patients [28]. The present study shows that CBCT with a voxel size of 0.30 mm and relatively little radiation is sufficient to represent the morphology of the alveolar crest compared to the gold standard. Furthermore, the position of the alveolar crest can be identified to help locate the coronal margin of PDL.

Many previous studies have focused on factors influencing the accuracy of CBCT datasets regarding the 3D reconstruction measurements[29-31] or the alveolar bone linear measurements such as alveolar bone level on the sagittal plane[28, 32-34]. Some studies have shown that a smaller voxel size is associated with better spatial resolution [29, 30], while others have concluded that there is no significant difference between CBCT with high-resolution and low-resolution protocols [31, 32]. A lower resolution also results in higher levels of image noise and influences the accuracy of alveolar bone measurements [33, 35]. This may explain the divergence in conclusions to some extent. Moreover, various factors of CBCT exposure parameters may influence image quality, such as the FOV and presence of metallic restorations [36, 37]. In this study, the FOV, voltage, and other conditions were controlled to investigate the effects of the voxel size. Additionally, all patients had metal brackets because CBCT was performed during orthodontic treatment, which is common in clinical situations. Although CBCT can provide an accurate 3D view of tooth roots and alveolar bone, dense intraoral metal brackets can severely compromise the image quality of crowns [38]. Therefore, in this study, intraoral optical scans were used to obtain profiles of anterior tooth crowns and surrounding soft tissue in STL format, eliminating the impact of metal artefacts on crown morphology.

The method for measuring the VBL on the sagittal plane of CBCT images to evaluate the periodontal situation has been well established [7-9]. Previous studies have reported that accurate, reliable and reproducible 3D models of the whole teeth could be generated with an intraoral scan superimposed over the CBCT imaging during the orthodontic treatment with the presence of brackets[39-41]. Further, the maximum inaccuracy was mainly found at the cervical margins when reconstructing lower anterior teeth models using CBCT dataset[42]. In this study, the brackets were chosen as reference marks to evaluate the alveolar bone crest. Our results showed that except for those at the labial midpoint, the digital VBL measurements of the lower anterior teeth

were significantly smaller than the intraoperative VBL measurements, while there was no significant difference in the BBD at any site between the two methods, which indicates that the main source of VBL measurement deviation was CEJ point selection. The positioning of the lower anterior CEJ on the 3D model tends to be gingivally oriented. Previously, Tong Wang et al [26] applied CBCT reconstruction to determine the RSA of extracted teeth in vitro. They found that the reconstruction of the crown and root still showed a clear CEJ boundary and a smooth area on the surface. Our study, however, indicated that the CEJ may not be an accurate or reproducible anatomical landmark for examining the periodontal health status of mandibular anterior teeth in vivo using a 3D model. This finding agrees with the observation reported by Marko Kuralt et al [43], who investigated the precision of gingival recession measurements and found that CEJ point selection was the main source of variability in measurements obtained from an intraoral optical scan-derived model. The reasons for the inaccurate positioning of the CEJ and the difficulty of its identification in this study may be the flatter morphology of the lower anterior teeth on the labial side and wear of the CEJ [44]. Further, the maximum inaccuracy was mainly found at the cervical margins when reconstructing lower anterior teeth models using CBCT dataset[42]. Therefore, when using the CEJ as an anatomical landmark to examine the periodontal health status of lower anterior teeth based on a 3D model, the possibility of underestimating the severity of alveolar bone loss should be considered. For non-orthodontic patients without brackets, other reference marks of lower anterior teeth with good reconstruction accuracy[42] such as root apex could be chosen to evaluate the periodontal bone level.

Since the gold standard for this study was the periodontal probe measurements, precision to ±1 mm with a manual periodontal probe was acceptable. The results showed a high diagnostic coincidence rate (>90%) in the maxilla and a relatively low diagnostic coincidence rate in the mandible. The Bland–Altman method showed that the limits of agreement were -1 mm to 1 mm for maxillary anterior teeth, which is generally consistent with the results of a previous study [32]. However, the broader limits of agreement and the wider span of differences in digital measurements of mandibular anterior teeth indicate that although both the maxillary and mandibular models are similarly accurate regarding the BBD measurements, the mandibular models are less reliable. This might be explained by the fact that skeletal class III patients have thinner anterior alveolar bone and more vertical bone loss than class I patients with normal occlusion[8] and that it is difficult to accurately measure the boundary of thin alveolar bone using CBCT, even with a 0.125-mm-voxel protocol [32].

This study presents a feasible and nondestructive method of obtaining in vivo PDL measurements from a digital model. Previous studies [5, 10, 11, 14, 45] have simulated VBL recession in vitro and assumed equal alveolar bone height loss at different sites around teeth, which does not truly reflect clinical periodontal conditions. Some researchers have used dry skulls; however, the lack of soft tissue would likely facilitate the detection of bone surfaces, which has been acknowledged to be a serious limitation [33]. Researchers have also used intact

cadaver heads with soft tissue for their studies; however, the lack of noise in radiological data normally created by patient movement probably contributes to improved results [32, 34, 46]. Although the clinical direct measuring and access has a great advantage, in this study, the intraoperative measurements routinely used in our facility for research purposes are not of the most accurate way in the interest of patient safety during the surgery and in an effort to keep examining time as short as diagnostically acceptable, the limitation should not be ignored. Moreover, though the accuracy of PDL measurements based on a 3D model has been identified, further validation with standardized measurements in larger sample sizes is needed. The fact that the lingual side cannot be observed under direct vision for locating measuring sites should not be ignored; the measurements in this study mainly focused on the morphological characteristics of alveolar dehiscence rather than fenestration.

Even with the limitations mentioned above, the current study introduces an accurate and consistent method to obtain PDL measurements from a reconstructed 3D model, which has important implications for clinical treatment. The 3D morphology of the PDL is a significant prognostic indicator in patients with periodontal disease or those undergoing orthodontic therapy, especially those with previous periodontal bone loss.

Conclusions

This study introduced a method to obtain PDL measurements from 3D reconstructions of in vivo CBCT scans. The results showed that CBCT with a voxel size of 0.3 mm reliably provided accurate data regarding the alveolar crest morphology for upper anterior teeth; acquiring these measurements with this method may allow periodontal conditions to be assessed more thoroughly and comprehensively.

Reference

1. Beertsen W, McCulloch CA, Sodek J. The periodontal ligament: a unique, multifunctional connective tissue. Periodontol 2000. 1997;13:20-40.
2. de Jong T, Bakker AD, Everts V, Smit TH. The intricate anatomy of the periodontal ligament and its development: Lessons for periodontal regeneration. J Periodontal Res. 2017;52(6):965-74.
3. Jiang N, Guo W, Chen M, Zheng Y, Zhou J, Kim SG, et al. Periodontal Ligament and Alveolar Bone in Health and Adaptation: Tooth Movement. Front Oral Biol. 2016;18:1-8.
4. Proffit WR. Contemporary orthodontics. 6th edition. ed. Philadelphia, IL: Elsevier; 2018.
5. Park SB, An SY, Han WJ, Park JT. Three-dimensional measurement of periodontal surface area for quantifying inflammatory burden. J Periodontal Implant Sci. 2017;47(3):154-64.
6. Lindskog S, Pierce AM, Blomlof L, Hammarstrom L. The role of the necrotic periodontal membrane in cementum resorption and ankylosis. Endod Dent Traumatol. 1985;1(3):96-101.
7. Lee S, Hwang S, Jang W, Choi YJ, Chung CJ, Kim KH. Assessment of lower incisor alveolar bone width using cone-beam computed tomography images in skeletal Class III adults of different vertical patterns. Korean J Orthod. 2018;48(6):349-56.
8. Kook YA, Kim G, Kim Y. Comparison of alveolar bone loss around incisors in normal occlusion samples and surgical skeletal class III patients. Angle Orthod. 2012;82(4):645-52.
9. Fleiner J, Hannig C, Schulze D, Stricker A, Jacobs R. Digital method for quantification of

circumferential periodontal bone level using cone beam CT. Clin Oral Investig. 2013;17(2):389-96.
10. Hong HH, Hong A, Huang YF, Liu HL. Incompatible amount of 3-D and 2-D periodontal attachments on micro-CT scanned premolars. PLoS One. 2018;13(3):e0193894.
11. Hong HH, Chang CC, Hong A, Liu HL, Wang YL, Chang SH, et al. Decreased Amount of Supporting Alveolar Bone at Single-Rooted Premolars Is Under Estimated by 2D Examinations. Sci Rep. 2017;8:45774.
12. Klock KS, Gjerdet NR, Haugejorden O. Periodontal attachment loss assessed by linear and area measurements in vitro. J Clin Periodontol. 1993;20(6):443-7.
13. Hujoel PP. A meta-analysis of normal ranges for root surface areas of the permanent dentition. J Clin Periodontol. 1994;21(4):225-9.
14. Gu Y, Tang Y, Zhu Q, Feng X. Measurement of root surface area of permanent teeth with root variations in a Chinese population-A micro-CT analysis. Arch Oral Biol. 2016;63:75-81.
15. Al-Rawi B, Hassan B, Vandenberge B, Jacobs R. Accuracy assessment of three-dimensional surface reconstructions of teeth from cone beam computed tomography scans. J Oral Rehabil. 2010;37(5):352-8.
16. Wang Y, He S, Guo Y, Wang S, Chen S. Accuracy of volumetric measurement of simulated root resorption lacunas based on cone beam computed tomography. Orthod Craniofac Res. 2013;16(3):169-76.
17. Tasanapanont J, Apisariyakul J, Wattanachai T, Sriwilas P, Midtbo M, Jotikasthira D. Comparison of 2 root surface area measurement methods: 3-dimensional laser scanning and cone-beam computed tomography. Imaging Sci Dent. 2017;47(2):117-22.
18. Palkovics D, Mangano FG, Nagy K, Windisch P. Digital three-dimensional visualization of intrabony periodontal defects for regenerative surgical treatment planning. BMC Oral Health. 2020;20(1):351.
19. Tayman MA, Kamburoglu K, Kucuk O, Ates FSO, Gunhan M. Comparison of linear and volumetric measurements obtained from periodontal defects by using cone beam-CT and micro-CT: an in vitro study. Clin Oral Investig. 2019;23(5):2235-44.
20. Mito T, Sato K, Mitani H. Cervical vertebral bone age in girls. Am J Orthod Dentofacial Orthop. 2002;122(4):380-5.
21. Vasir NS, Thompson RT, Davies TM. Dental and skeletal changes following sagittal split osteotomy for correction of mandibular prognathism. Eur J Orthod. 1991;13(2):134-42.
22. Forst D, Nijjar S, Flores-Mir C, Carey J, Secanell M, Lagravere M. Comparison of in vivo 3D cone-beam computed tomography tooth volume measurement protocols. Prog Orthod. 2014;15:69.
23. Jing W-d, Jiao J, Xu L, Hou J-x, Li X-t, Wang X-x, et al. Periodontal soft- and hard-tissue changes after augmented corticotomy in Chinese adult patients with skeletal Angle Class III malocclusion: A non-randomized controlled trial. Journal of Periodontology. 2020;91(11):1419-28.
24. Scarfe WC, Azevedo B, Pinheiro LR, Priaminiarti M, Sales MAO. The emerging role of maxillofacial radiology in the diagnosis and management of patients with complex periodontitis. Periodontol 2000. 2017;74(1):116-39.
25. Kim DM, Bassir SH. When Is Cone-Beam Computed Tomography Imaging Appropriate for Diagnostic Inquiry in the Management of Inflammatory Periodontitis? An American Academy of Periodontology Best Evidence Review. J Periodontol. 2017;88(10):978-98.
26. Wang T, Pei X, Luo F, Jia L, Qin H, Cheng X, et al. Evaluation of tooth root surface area using a three-dimensional scanning technique and cone beam computed tomographic reconstruction in vitro. Arch Oral Biol. 2017;84:13-8.
27. Choi IGG, Cortes ARG, Arita ES, Georgetti MAP. Comparison of conventional imaging techniques and CBCT for periodontal evaluation: A systematic review. Imaging Sci Dent. 2018;48(2):79-86.
28. Spin-Neto R, Gotfredsen E, Wenzel A. Impact of voxel size variation on CBCT-based diagnostic outcome in dentistry: a systematic review. J Digit Imaging. 2013;26(4):813-20.
29. Maret D, Telmon N, Peters OA, Lepage B, Treil J, Inglese JM, et al. Effect of voxel size on the accuracy of 3D reconstructions with cone beam CT. Dentomaxillofac Radiol. 2012;41(8):649-55.
30. Dong T, Yuan L, Liu L, Qian Y, Xia L, Ye N, et al. Detection of alveolar bone defects with three

different voxel sizes of cone-beam computed tomography: an in vitro study. Sci Rep. 2019;9(1):8146.
31. Sang YH, Hu HC, Lu SH, Wu YW, Li WR, Tang ZH. Accuracy Assessment of Three-dimensional Surface Reconstructions of In vivo Teeth from Cone-beam Computed Tomography. Chin Med J (Engl). 2016;129(12):1464-70.
32. Patcas R, Muller L, Ullrich O, Peltomaki T. Accuracy of cone-beam computed tomography at different resolutions assessed on the bony covering of the mandibular anterior teeth. Am J Orthod Dentofacial Orthop. 2012;141(1):41-50.
33. Sun Z, Smith T, Kortam S, Kim DG, Tee BC, Fields H. Effect of bone thickness on alveolar bone-height measurements from cone-beam computed tomography images. Am J Orthod Dentofacial Orthop. 2011;139(2):e117-27.
34. Wood R, Sun Z, Chaudhry J, Tee BC, Kim DG, Leblebicioglu B, et al. Factors affecting the accuracy of buccal alveolar bone height measurements from cone-beam computed tomography images. Am J Orthod Dentofacial Orthop. 2013;143(3):353-63.
35. de-Azevedo-Vaz SL, Vasconcelos Kde F, Neves FS, Melo SL, Campos PS, Haiter-Neto F. Detection of periimplant fenestration and dehiscence with the use of two scan modes and the smallest voxel sizes of a cone-beam computed tomography device. Oral Surg Oral Med Oral Pathol Oral Radiol. 2013;115(1):121-7.
36. Icen M, Orhan K, Seker C, Geduk G, Cakmak Ozlu F, Cengiz MI. Comparison of CBCT with different voxel sizes and intraoral scanner for detection of periodontal defects: an in vitro study. Dentomaxillofac Radiol. 2020;49(5):20190197.
37. Pauwels R, Faruangsaeng T, Charoenkarn T, Ngonphloy N, Panmekiate S. Effect of exposure parameters and voxel size on bone structure analysis in CBCT. Dentomaxillofac Radiol. 2015;44(8):20150078.
38. Harris BT, Montero D, Grant GT, Morton D, Llop DR, Lin WS. Creation of a 3-dimensional virtual dental patient for computer-guided surgery and CAD-CAM interim complete removable and fixed dental prostheses: A clinical report. J Prosthet Dent. 2017;117(2):197-204.
39. Lim SW, Moon RJ, Kim MS, Oh MH, Lee KM, Hwang HS, et al. Construction reproducibility of a composite tooth model composed of an intraoral-scanned crown and a cone-beam computed tomography-scanned root. Korean J Orthod. 2020;50(4):229-37.
40. Lee RJ, Weissheimer A, Pham J, Go L, de Menezes LM, Redmond WR, et al. Three-dimensional monitoring of root movement during orthodontic treatment. Am J Orthod Dentofacial Orthop. 2015;147(1):132-42.
41. Lee RJ, Pham J, Choy M, Weissheimer A, Dougherty HL, Jr., Sameshima GT, et al. Monitoring of typodont root movement via crown superimposition of single cone-beam computed tomography and consecutive intraoral scans. Am J Orthod Dentofacial Orthop. 2014;145(3):399-409.
42. Maret D, Peters OA, Galibourg A, Dumoncel J, Esclassan R, Kahn JL, et al. Comparison of the accuracy of 3-dimensional cone-beam computed tomography and micro-computed tomography reconstructions by using different voxel sizes. J Endod. 2014;40(9):1321-6.
43. Kuralt M, Gaspersic R, Fidler A. The precision of gingival recession measurements is increased by an automated curvature analysis method. BMC Oral Health. 2021;21(1):505.
44. Pini-Prato G, Franceschi D, Cairo F, Nieri M, Rotundo R. Classification of dental surface defects in areas of gingival recession. J Periodontol. 2010;81(6):885-90.
45. Gu Y, Zhu Q, Tang Y, Zhang Y, Feng X. Measurement of root surface area of permanent teeth in a Chinese population. Arch Oral Biol. 2017;81:26-30.
46. Damstra J, Fourie Z, Huddleston Slater JJ, Ren Y. Accuracy of linear measurements from cone-beam computed tomography-derived surface models of different voxel sizes. Am J Orthod Dentofacial Orthop. 2010;137(1):16 e1-6; discussion -7.

Figures

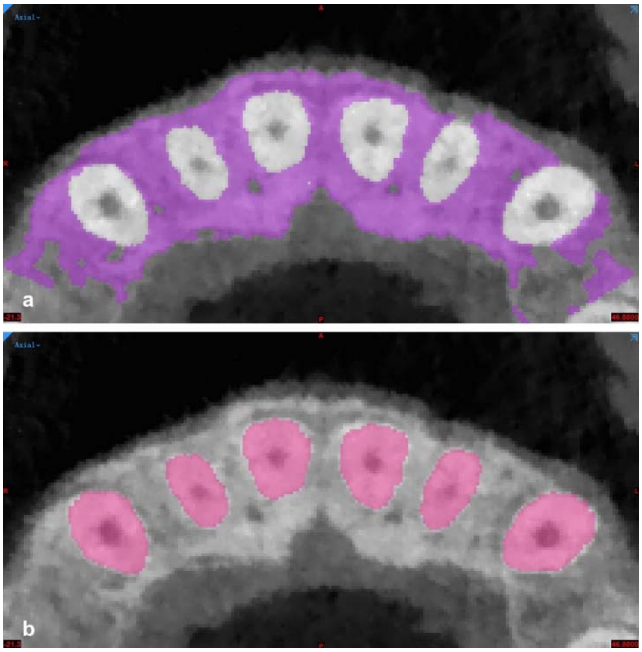

Figure 1. Process of segmenting alveolar bone and teeth in Mimics. **a** Manual alveolar bone segmentation, **b** Manual teeth segmentation

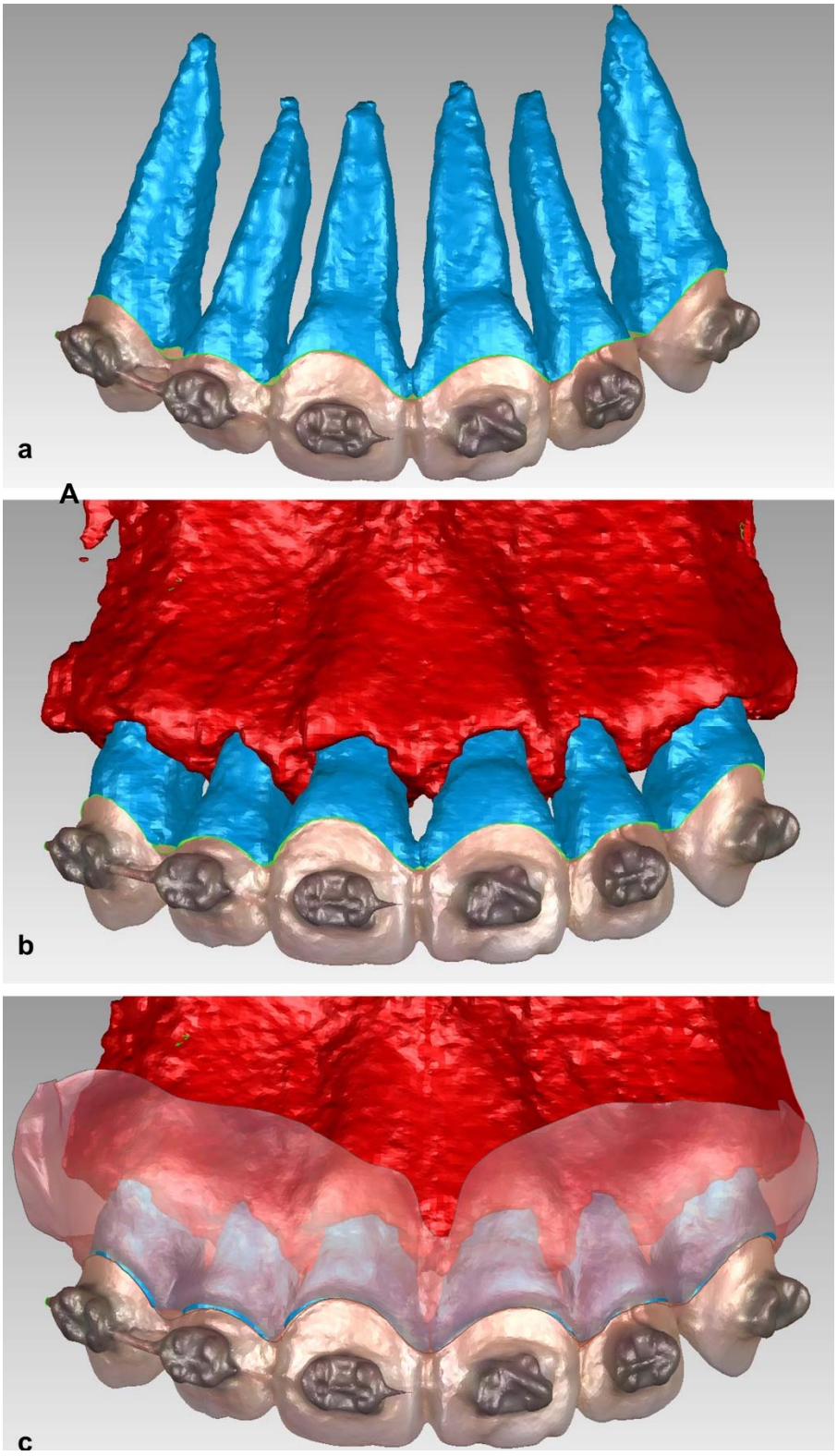

Figure 2. Digital teeth, bone and soft tissue models in Geomagic. **a** Digital teeth models with an intraoral scan superimposed over the crowns, **b** Digital teeth and bone models, **c** Digital teeth and bone models generated from CBCT datasets, soft tissue model derived from an intraoral scan

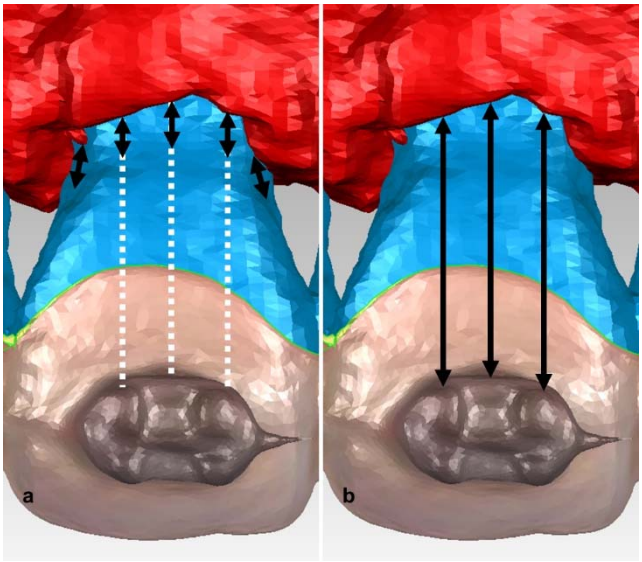

Figure 3. Digital linear measurements. **a** VBL measurements at mesiolabial, mesiobracket, midlabial, distobracket, and distolabial sites, **b** BBD measurements at mesiobracket, midlabial, and distobracket sites

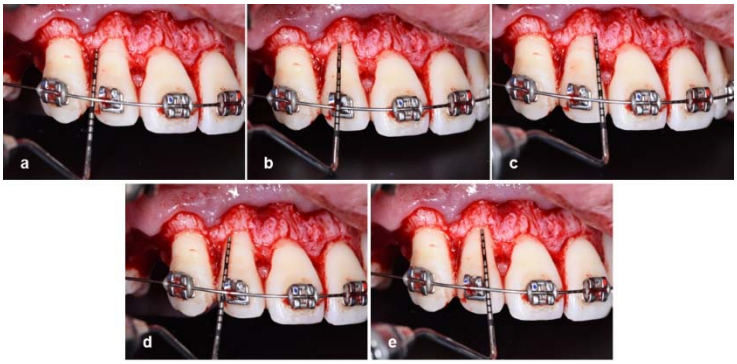

Figure 4. Intrasurgical linear measurements. **a, b, c** Linear measurements at distolabial, midlabial and mesiolabial sites, **d, e** Linear measurements at mesiobracket and distobracket sites

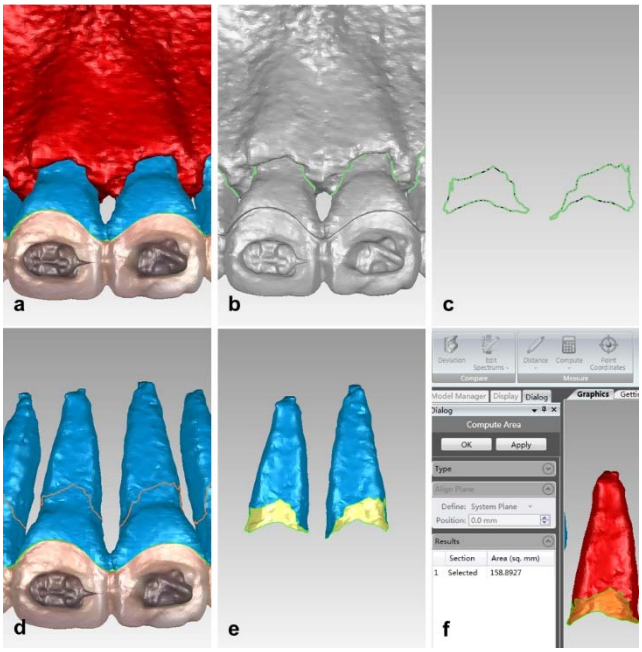

Figure 5. Establishment of PDL digital models. **a** Teeth and alveolar bone digital models, **b** The alveolar bone crests were drawn on the teeth models, **c** The alveolar bone crests curves, **d** The teeth models were separated along the alveolar bone crests curves, **e** The PDL digital models, **f** Computing PDL area

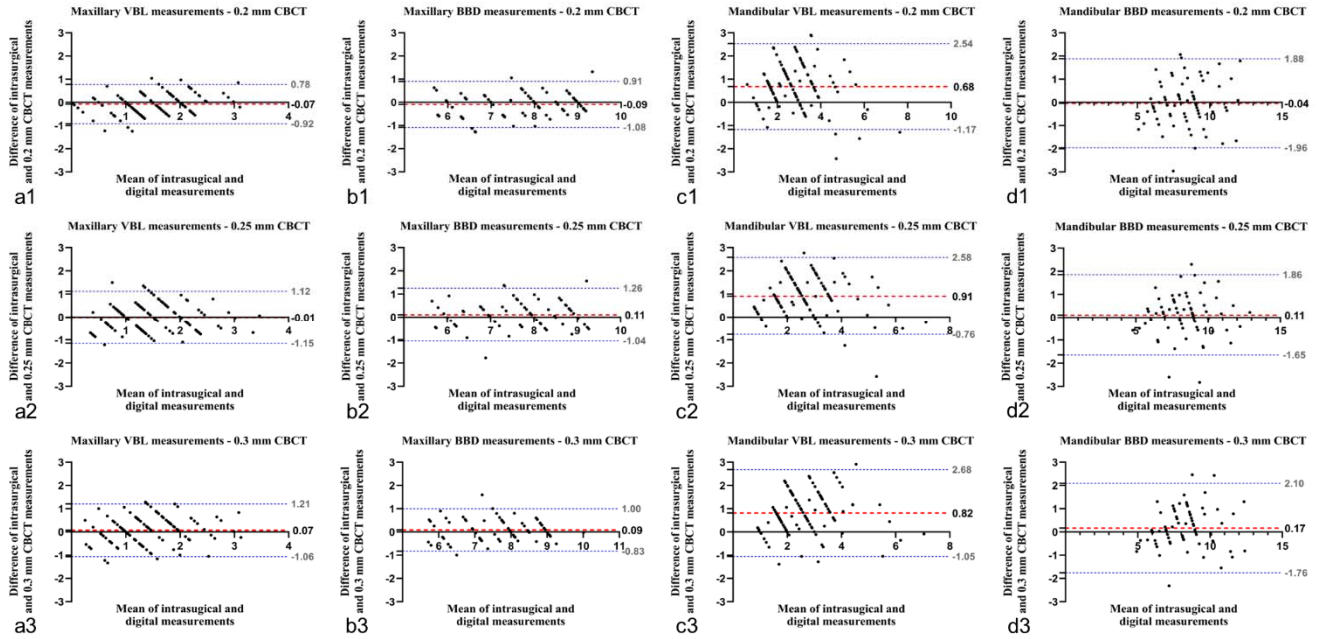

Figure 6. Bland-Altman plots of intrasurgical and digital linear measurements with different CBCT voxel sizes. The difference against the mean and the limits of agreement are shown. **a1 ~ a3** VBL measurements of maxillary anterior teeth with different CBCT voxel sizes, **b1 ~ b3** BBD measurements of maxillary anterior teeth with different CBCT voxel sizes, **c1 ~ c3** VBL measurements of mandibular anterior teeth with different CBCT voxel sizes, **d1 ~ d3** BBD measurements of mandibular anterior teeth with different CBCT voxel sizes

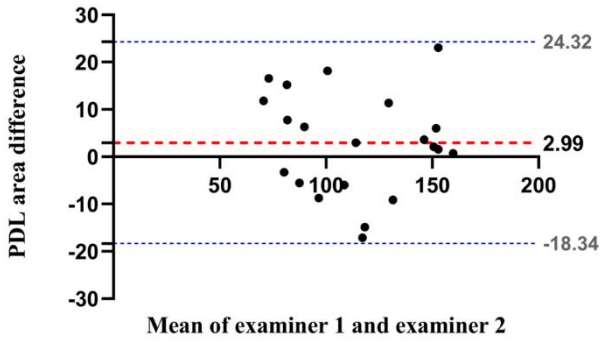

Figure 7. Bland-Altman plots of PDL area measurements between examiner 1 and examiner 2.

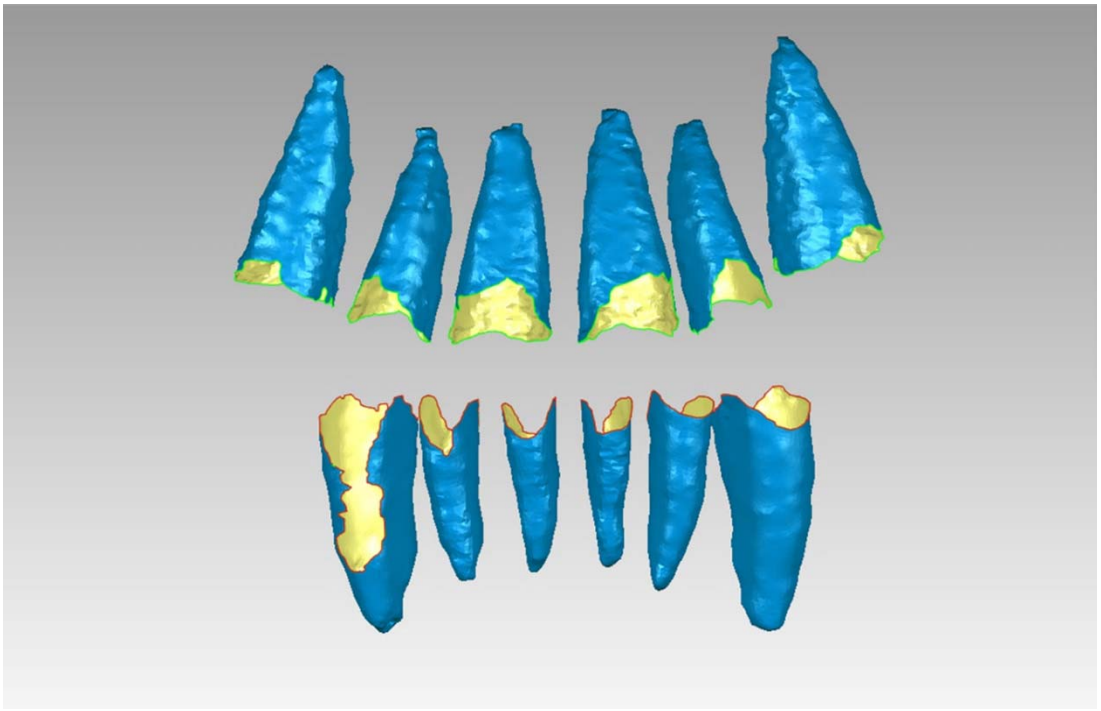

Figure 8. An example of PDL models.

Tables

Table 1. Comparison of intrasurgical and digital linear measurements at different sites with different voxel sizes

Measurements	Digital						Intrasurgical			
	0.2mm		0.25mm		0.3mm					
Maxillary anterior teeth	Mean	SD	Mean	SD	Mean	SD	Mean	SD	P	Multiple Comparison
VBL_Mla (mm)	1.08	0.50	1.06	0.44	1.01	0.47	1.00	0.74	0.22	——
VBL_MB (mm)	1.58	0.53	1.49	0.72	1.39	0.54	1.46	0.66	0.74	——
VBL_La (mm)	1.98	0.57	2.04	0.74	1.93	0.69	1.79	0.72	0.63	——
VBL_DB (mm)	1.68	0.47	1.52	0.59	1.51	0.54	1.60	0.63	0.71	——
VBL_Dla (mm)	1.41	0.63	1.16	0.75	1.01	0.55	1.35	0.76	0.15	——
BBD_MB (mm)	7.47	1.08	7.27	1.07	7.32	0.99	7.33	1.11	0.92	——
BBD_La (mm)	8.09	0.91	7.86	1.03	7.81	1.04	7.96	1.21	0.81	——
BBD_DB (mm)	7.77	0.97	7.32	0.95	7.36	0.98	7.63	0.94	0.32	——
Mandibular anterior teeth										
VBL_Mla (mm)	1.56	0.60	1.30	0.45	1.55	0.57	2.13	0.76	0.000**	intra> (0.2mm, 0.25mm, 0.3mm)
VBL_MB (mm)	2.54	0.86	2.37	0.79	2.48	0.84	3.31	0.70	0.000**	intra> (0.2mm, 0.25mm, 0.3mm)
VBL_La (mm)	3.87	1.72	3.69	1.40	3.65	1.56	4.52	1.05	0.15	——
VBL_DB (mm)	2.75	0.86	2.47	1.16	2.39	0.62	3.44	0.97	0.000**	intra> (0.2mm, 0.25mm, 0.3mm)
VBL_Dla (mm)	1.50	0.58	1.27	0.46	1.51	0.54	2.25	0.81	0.000**	intra> (0.2mm, 0.25mm, 0.3mm)
BBD_MB (mm)	8.16	1.56	8.01	1.54	7.94	1.50	7.92	1.59	0.95	——
BBD_La (mm)	9.36	2.23	9.42	2.00	9.24	2.20	9.35	1.60	0.99	——
BBD_DB (mm)	8.09	1.52	8.01	1.84	7.78	1.40	7.98	1.77	0.92	——

P, One-way ANOVA with Duncan's multiple comparison test was performed for comparison between intrasurgical and digital linear measurements.

*, P≤0.05; **, P≤0.01

Table 2. Intraclass correlation coefficient (ICC) analysis of intrasurgical and digital linear measurements with different voxels

		0.2mm			0.25mm			0.3mm		
		Intraclass correlation (ICC)	95% CI		Intraclass correlation (ICC)	95% CI		Intraclass correlation (ICC)	95% CI	
	Measurements		Lower bound	Upper bound		Lower bound	Upper bound		Lower bound	Upper bound
Maxillary anterior teeth	VBL	0.793**	0.715	0.851	0.684**	0.576	0.769	0.646**	0.528	0.739
	BBD	0.887**	0.825	0.928	0.850**	0.771	0.904	0.908**	0.857	0.942
Mandibular anterior teeth	VBL	0.726**	0.629	0.801	0.769**	0.684	0.833	0.689**	0.582	0.772
	BBD	0.839**	0.754	0.896	0.872**	0.803	0.918	0.842**	0.758	0.898

*, P≤0.05; **, P≤0.01

Table 3. Descriptive statistics, Diagnostic coincidence rates, limits of agreement and 95% CI values for linear measurement differences with different voxel sizes of maxillary anterior teeth

Measurement difference	Mean difference (mm)	Median (mm)	SD (mm)	Range (mm)	Diagnostic coincidence rates	Limits of agreement (mm)	95%CI (mm)
VBL (n=120)							
0.2mm	-0.07	-0.10	0.43	2.28	96.66%	(-0.92 - 0.78)	（-0.15 - 0.004）
0.25mm	-0.01	-0.01	0.58	2.72	92.50%	(-1.15 - 1.12)	(-0.11 - 0.09)
0.3mm	0.07	0.09	0.58	2.61	90.00%	(-1.06 - 1.21)	(-0.03 - 0.17)
BBD (n=72)							
0.2mm	-0.09	0.01	0.51	2.60	90.27%	(-1.08 - 0.91)	(-0.21 - 0.03)
0.25mm	0.11	0.11	0.59	3.34	94.44%	(-1.04 - 1.26)	(-0.03 - 0.25)
0.3mm	0.09	0.02	0.47	2.59	97.22%	(-0.82 - 1.00)	(-0.02 - 0.19)

Table 4. Descriptive statistics, Diagnostic coincidence rates, limits of agreement and 95% CI values for linear measurement differences with different voxel sizes of mandibular anterior teeth

Measurement Difference	Mean difference (mm)	Median (mm)	SD (mm)	Range (mm)	Diagnostic coincidence rates	Limits of agreement (mm)	95%CI (mm)
VBL (n=120)							
0.2mm	0.68	0.71	0.95	5.82	63.33%	(-1.17 - 2.54)	(0.51 - 0.85)
0.25mm	0.91	0.88	0.85	5.92	56.66%	(-0.76 - 2.58)	(0.75 - 1.06)
0.3mm	0.82	0.81	0.95	6.58	56.66%	(-1.05 - 2.68)	(0.64 - 0.98)
BBD (n=72)							
0.2mm	-0.04	-0.10	0.98	5.03	66.67%	(-1.96 - 1.88)	(-0.26 - 0.19)
0.25mm	0.11	0.20	0.89	5.13	77.78%	(-1.65 - 1.86)	(-0.10 - 0.31)
0.3mm	0.17	0.08	0.98	6.23	70.83%	(-1.76 - 2.10)	(-0 06 - 0.40)